

การศึกษากระบวนการดัดของอลูมิเนียมแผ่นบางโดยวิธีการดัดแบบสามจุด โดยวิธีไฟไนต์อีเลเมนต์

Finite Element Simulation of Bending Process Under Three-Point Bending Test of Aluminum Sheet

Weerayut Jina^{1*}, Somjet Thanomputra¹, Montri Sangsuriyun², Shigeru Nagasawa^{3,4}

¹ Department of Mechanical and Manufacturing Engineering, Faculty of Science and Engineering, Kasetsart University, Chalermphrakiat Sakon Nakhon Province Campus, weerayut.j@ku.th, somjet.tha@ku.th

² Department of Industrial Engineering, Faculty of Engineering, Nakhon Phanom University, montri.sang@npu.ac.th

³ Department of Mechanical Engineering, Nagaoka University of Technology

⁴ Faculty of Engineering, Sanjo City University, nagasawa.shigeru@sanjo-u.ac.jp

Abstract

The aim of this work is to describe the bending behavior under the three-point bending test of an aluminum alloy thin sheet A1050P by investigating the maximum principal stress and the deformation characteristics through the finite element method (FEM). The three-point bending test apparatus was experimentally examined with a 0.39-mm thickness aluminum sheet. To verify the bending mechanics of the bending part of an aluminum sheet with the FEM model, the initial displacement of punch d_p was varied within a certain range, and the experimental result was investigated by the FEM model. The FEM model of three-point bending was developed and simulated using isotropic elasto-plastic solid properties. When investigating the three-point bending process of an aluminum sheet on the FEM model, the friction coefficient of the tools and an aluminum sheet seems to be the primary characteristic to close to the experimental result. Through the FEM simulation of the bending part of an aluminum sheet, the following results were revealed: (1) The simulated bending force b_F seems to increase with the friction coefficient when the displacement of the punch $d_p > 0.5\text{mm}$. (2) The contact friction coefficient of the die was higher than that of the punch. (3) The minimum principal stress s_{p2} (as a compressive state) was higher than that of the maximum principal stress s_{p1} (as a tensile state).

Keywords: Three point bending test; Bending behavior of A1050P; FEM

1. Introduction

Aluminum alloy thin sheet A1050P has high plasticity, electrical conductivity, corrosion resistance and good thermal conductivity characteristics. In this work, the three-point bending test was carried out of an aluminum sheet. The three-point bending test is one of the most important for material testing methods to explain the mechanical performance of materials in the manufacturing processes. The bending method is recently noticed in order to bend any shapes of precision parts such as a lead-frame of integrated circuits, it is commonly used in semiconductor packages. One of the most important things in the bending process is to estimate the bending deflection, bending strength, and bending fatigue Sun et al. (2012), Li et al. (2013). A 3-point bending test of titanium alloy are studied through experiment and simulation Maati et al. (2020).

Several research works Thuillier et al. (2010), Wagner et al. (2020), Yue et al. (2018), Hou et al. (2016) have studied experimentally and numerically the three-point bending test of an aluminum sheet.

Nowadays, many research works have studied an aluminum alloy thin sheet A1050P. Murayama et al. (2003) explained the effect of sheet thickness of an aluminum sheet and friction on load characteristic of crushed center bevel cutter indented to an aluminum sheet. Murayama et al. (2004) investigated the relationship between thickness of wedged sheet and tip thickness of crushed cutter. CHAIJIT et al. (2006) investigated the critical condition for cutting off the aluminum sheet. CHAIJIT et al. (2009) studied the sensitivity of crack propagation of an aluminum worksheet during wedge shearing process. Ould Ouali et al. (2009) studied the rolling of a A1050P aluminum sheet. Chakravarty et al. (2022) The estimated the distribution of dislocation density at the mid thickness of 1050 Al alloy. The dislocation density at the mid thickness of an aluminum alloy 1050 was estimated by Chakravarty et al. (2022). Salem et al.

(2022) predicted the springback of Aluminum 1050 A during the air v-bending process.

In this report, the simulation bending model was compared to the experimental result, and the bending strength was investigated, in order to reveal the maximum-minimum principal stresses and the estimation of the contact friction force of an aluminum sheet during the three-point bending test between the punch and dies. The simulation model was varied the friction coefficient in order to validate the experimental three-point bending test.

2. Methodology

2.1 Materials

A commercially pure aluminum alloy sheet (JIS-A1050P) of 0.39 mm thickness was carried out in the three-point bending experiment. The tensile properties of the aluminum sheet for transverse direction are shown in Table 1.

Table 1 Mechanical properties of aluminum sheets (A1050P), CHAIJIT et al. (2009).

Thickness t [mm]	0.39
Young's modulus E [GPa]	78.6
Yield Stress s_y [MPa]	140
Ultimate tensile strength s_B [MPa]	150
Plastic coefficient, F [MPa]	90
Work hardening exponent, n	0.46

2.2 Experimental method

The out-of-plane three-point bending experiments were carried out under the standard test (based on ASTM-D790-3. (2003)) as shown in Figure 1. Specimens were prepared 5 pieces as a square sheet with a width of the specimen $W_s = 20\text{mm}$ (transverse direction), a length of the specimen $l_w = 20\text{mm}$ (longitudinal direction), and the thickness of 0.39 mm. The span length of die l_s was 4mm, and both sides of corner radii r_c were 0.3mm. The radii of punch r_p was 0.95mm, and thickness of punch t_p was 1.9mm. The upper crosshead had a punch/indenter mounted on a

load cell. The aluminum sheet was placed onto the die on both sides. The displacement of punch d_p moved downward with a velocity $V = 0.1 \text{ mm s}^{-1}$. The punch direction angle f was chosen as 90° with respect to the rolling direction of worksheet (RD), as shown in Figure 2. The bending force b_f and the d_p were automatically measured using a load cell and linear gauge sensor. The specimen and both sides of the die, the tool surface were washed with alcohol before the three-point bending test. The deformation profile of bending part was observed by a CCD camera during bending the aluminum sheet.

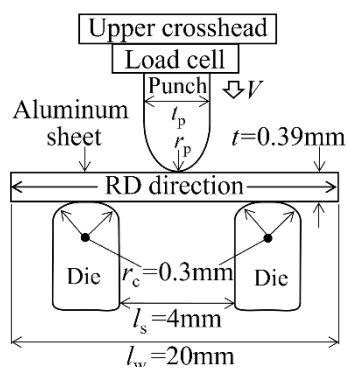


Figure 1 Schematic of the three point bending apparatus.

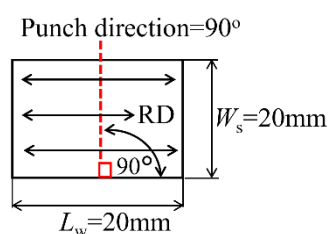


Figure 2 Punch direction of specimen.

2.3 Simulation method

To validate the experimental result, the simulation model was carried out as shown in Figure 3. The simulation model was the same as that of the experiment as illustrated in Figure 1. To estimate the behavior of three-point bending mechanism under the bending stage of an aluminum sheet (JIS-A1050P). A general-purpose finite element code, MSC.MARC was employed for

simulating the three-point bending process. The updated Lagrange method and a large strain state were used for analyzing a two-dimensional model (plane strain). The deformable body of the worksheet was presumed to be an isotropic, elastoplastic material conforming to the isotropic hardening power law $s = Fe^{-n}$. Herein, the value of $F = 140 \text{ MPa}$ (1.56 times of the s_y was assumed) and $n = 0.46$ were selected as described in section 2.1. During the three-point bending process, all elements were assumed to have no crack and no fracture. Therefore, the coulomb friction model was assumed for each contact surface, the friction coefficients between the deformable body and punch-dies were initially assumed to be 0.2 CHAJIT et al. (2009). Then the friction coefficients were assumed to be increased by 0.6, 0.8 and 1.6, respectively. The length of the deformable body was 20mm and the sheet thickness was $t = 0.39 \text{ mm}$. The movement of punches and dies was made of rigid bodies. The total number of nodes was 6510, while that of total divided elements of the worksheet was 5850. The punch was moved downward, while the both of dies were fixed. Each step of the punch was performed with 100 steps of total increment for simulating the three-point bending test.

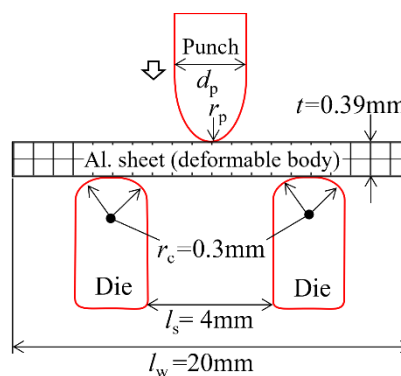


Figure 3 Schematic of the three-point bending apparatus for simulation model.

3. Results and discussion

3.1 Experimental results

Figure 4 shows the relationship between the bending force and displacement of the punch d_p , the bending force response was recorded for $d_p=0-2$ mm. Here the bending force b_F tended to be increased with the displacement of punch d_p .

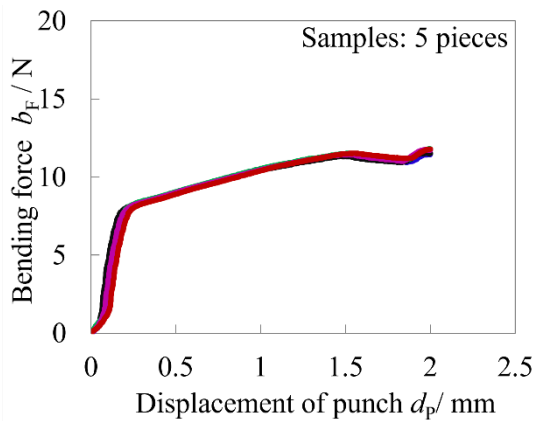
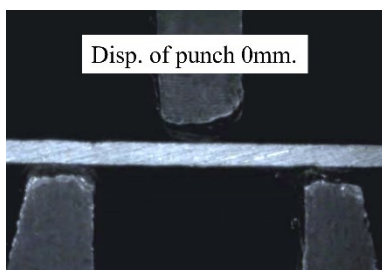
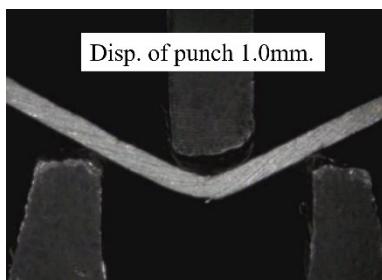


Figure 4 Relationship between bending force and displacement of punch d_p .

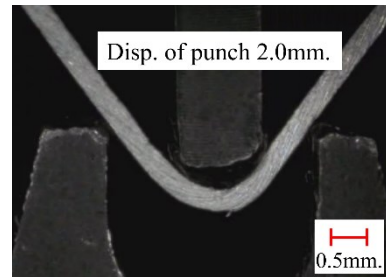
Figure 5 (a)-(c) shows the representative side-view photographs of bending specimens during three-point bending test under the bending state (for displacement of punch 0, 1 and 2mm).



(a) In case of the displacement of punch =0mm.



(b) In case of the displacement of punch =1.0mm.



(c) In case of the displacement of punch =2.0mm.

Figure 5 (a)-(c) Photographs of the side view of specimen during three-point bending test.

3.2 Simulation results

3.2.1 Effect of friction coefficients on bending load response.

Figure 6 “Sim.” shows the simulated relationship between the bending force b_F and displacement of punch d_p for $d_p =0-2$ mm when increasing the friction coefficients $m=0.2$ (based on CHAJIT et al. (2009)), 0.6, 0.8 and 1.6, while “Exp.” shows the experimental result. The simulated results were found that the b_F tended to be increased when the $d_p >0.6$ mm.

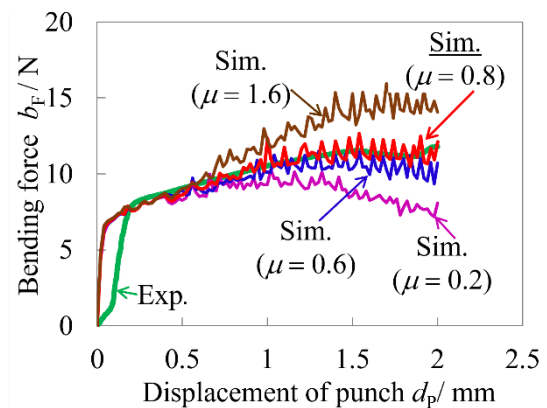


Figure 6 Relationship between bending force and displacement of punch d_p when increasing the friction coefficients (comparison of experimental with the simulated result).

As for the mismatching between the simulated and experimental results at the initial state when $d_p <0.2$ mm due to the initial state of the three-point bending experiment, the sliding occurred between the worksheet and tools (punch and dies). As the results in Figure 6 indicate, it was found that the

simulated cases of $m=0.8$ was fairly similar to the experimental result. Hence, the $m=0.8$ was performed to explain the three-point bending process.

Figure 7 shows a representation of the relationship between the contact friction force m_c and arc length when the d_p was moved downward at 1mm. Herein, the contact friction force of dies m_d versus the worksheet and the contact friction force of punch m_p versus the worksheet was shown. As a result, the contact friction force between the dies and worksheet was higher than that of the contact friction force between the punch and worksheet.

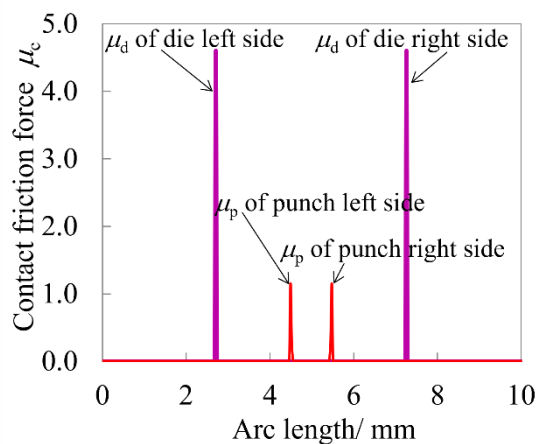


Figure 7 Relationship between the contact friction force m_c and arc length of worksheet during the three-point bending process on the simulation model at $d_p=1\text{mm}$.

3.2.2 Deformation characteristic under three-point bending simulation.

Figures 8 and 9 show the representative comparisons between the simulation and the experimental result. Herein, Figure 8 in the case of $d_p=1.0\text{mm}$ and Figure 9 in the case of $d_p=2.0\text{mm}$, respectively. The simulated result was fairly matched with the experimental result. As for the simulated result, the upper bound of contour band diagrams was based on yield stress ($s_y=140\text{MPa}$) as shown in Table 1. Therefore, the maximum principal stress s_{p1} (tensile state) was shown in the lower

side of the worksheet, while that of the minimum principal stress s_{p2} (compressive state) was established on the upper side of the worksheet.

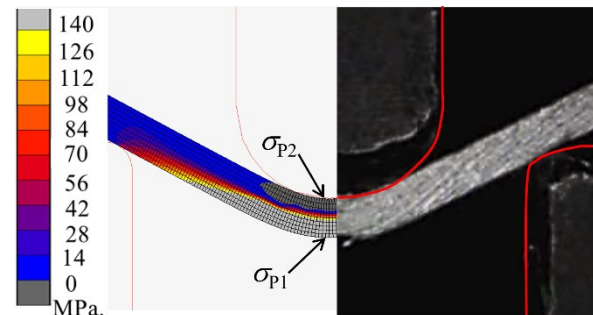


Figure 8 Contour band diagrams of 1st (maximum as a tensile state) s_{p1} and 2nd (minimum as a compressive state) s_{p2} principal stresses in case of $d_p=1.0\text{mm}$ (simulated result versus experimental result).

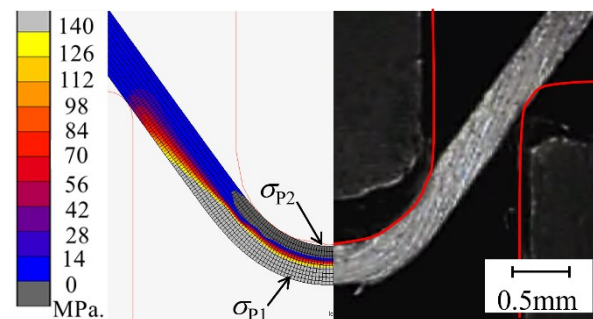


Figure 9 Contour band diagrams of 1st (maximum as a tensile state) s_{p1} and 2nd (minimum as a compressive state) s_{p2} principal stresses in case of $d_p=2.0\text{mm}$ (simulated result versus experimental result).

Figures 10 shows the relationship between the s_{p1} and s_{p2} principal stresses and the arc length in the case of $d_p=1.0$ and 2.0mm . The s_{p1} at $d_p=1.0$ was 237MPa and the s_{p1} at $d_p=2.0$ was 231MPa , while that of the case of the s_{p2} at $d_p=1.0$ was 272MPa and the s_{p2} at $d_p=2.0$ was 287MPa .

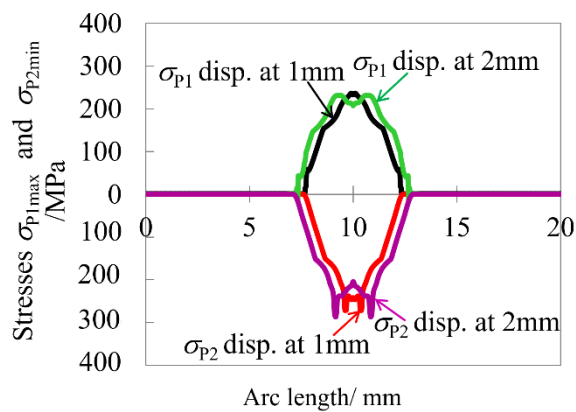


Figure 10 σ_{p1} (Max.) and σ_{p2} (Min). principal stresses on upper and lower surface.

4. Conclusion

The three-point bending test of $t=0.39\text{mm}$ thickness A1050P aluminum sheet was experimentally carried out in order to estimate the bending strength of the aluminum sheet. To discuss with the effect of the contact friction coefficients of the worksheet and tools, the deformation characteristic under the three-point bending process, and the maximum principal stress, an FEM simulation was also conducted by using the elastoplastic properties.

Through these works, the experimental and simulated results were summarized as follows:

- 1) Regarding the experimental results of the out-of-plane three-point bending test, the bending force b_F was quite increased with the linear tendency when the $d_p < 0.2\text{mm}$, while the $0.2 < d_p < 2\text{mm}$ the b_F was slightly increased with the increasing of the d_p .
- 2) The authors proposed a material model for the aluminum sheet bending analysis. In the FEM model, the 1.56 times of the tensile yield stress was assumed. As a result, the proposed simulation model was confirmed by a good fit between the simulated bending force and experimental bending force.
- 3) When verifying the friction coefficients $m=0.2-1.6$ through the FEM model, the b_F was increased when the $d_p > 0.6\text{mm}$, it was found that the simulated cases of $m=0.8$ was fairly matched to

the experimental result. When compared the contact friction force between the worksheet and the tools, it was indicated that the contact friction force between the worksheet and the dies was higher than that of the contact friction force between the punch and worksheet.

- 4) The maximum principal stress σ_{p1} (as a tensile state) was lower than that of the minimum principal stress σ_{p2} (as a compressive state).

5. Acknowledgements

This work was partially supported by Nagasawa laboratory from department of mechanical engineering, Nagaoka University of Technology, Japan for their support the MSC.MARC software and experimental apparatus.

6. References

- [1] CHAJIT, S., & S. NAGASAWA. 2009. FEM simulation on Sensitivity of Crack Propagation on Aluminum Sheet during Wedge Shearing Process. *Proceedings of International Conference on Leading Edge Manufacturing in 21st century : LEM21* 2009.5: p.379–384.
- [2] CHAJIT, S., N. SHIGERU, F. YASUSHI, M. MITSUHIRO, & K. ISAMU. 2006. EFFECT OF TIP PROFILE ON CUTTING PROCESSABILITY OF A TRAPEZOIDAL CUTTING BLADE INDENTED TO AN ALUMINUM SHEET. *JOURNAL OF MECHANICS OF MATERIALS AND STRUCTURES* 1(8): p.1301–1321.
- [3] Chakravarty, P., G. Pál, J.G. Bátorfi, & J.J. Sidor. 2022. Estimation of Dislocation Distribution at Mid Thickness for 1050 Al. *Acta Materialia Transylvanica* 5(1): p.6–9.
- [4] Hou, P. et al. 2016. Influence of punch radius on elastic modulus of three-point bending tests. *Advances in Mechanical Engineering* 8(5): p.1–8.
- [5] Li, A., J. Zhao, D. Wang, X. Gao, & H. Tang. 2013. Three-point bending fatigue behavior of WC – Co cemented carbides. *Materials and Design* 45:

- p.271–278.
- [6] Maati, A., L. Tabourot, P. Balland, & S. Belaid. 2020. Influence of the material microstructural properties on a 3-point bending test P. Le Grogne (ed). *Mechanics & Industry* 21(518): p.1–9.
- [7] Murayama, M., S. Nagasawa, Y. Fukuzawa, & I. Katayama. 2003. Effect of sheet thickness and friction on load characteristic of crushed center bevel cutter indented to aluminum sheet. *Computational and Experimental Methods* 8: p.115–124.
- [8] Murayama, M., S. Nagasawa, Y. Fukuzawa, & I. Katayama. 2004. Cutting mechanism and load characteristic of trapezoidal center bevel cutter indented on aluminum sheet. *JSME International Journal, Series C: Mechanical Systems, Machine Elements and Manufacturing* 47(1): p.21–28.
- [9] Ould Ouali, M., & M. Aberkane. 2009. Micromechanical modeling of the rolling of a A1050P aluminum sheet. *International Journal of Material Forming* 2(1): p.1–18.
- [10] Salem, C. Ben, & W. Meslameni. 2022. A Numerical Investigation on the Springback in Air V-Bending of Aluminum 1050 A. *International Journal of Research in Industrial Engineering* 11(2): p.119–133.
- [11] Sun, B., R. Liu, & B. Gu. 2012. Numerical simulation of three-point bending fatigue of four-step 3-D braided rectangular composite under different stress levels from unit-cell approach. *Computational Materials Science* 65: p.239–246.
- [12] Thuillier, S., N. Le Maoût, & P.Y. Manach. 2010. Bending Limit Prediction of an Aluminum Thin Sheet. *International Journal of Material Forming* 3(S1): p.223–226.
- [13] Wagner, L., P. Larour, D. Dolzer, F. Leomann, & C. Suppan. 2020. Experimental issues in the instrumented 3 point bending VDA238-100 test. *IOP Conference Series: Materials Science and Engineering* 967(1): p.1–11.
- [14] Yue, Z. et al. 2018. Springback prediction of aluminum alloy sheet under changing loading paths with consideration of the influence of kinematic hardening and ductile damage. *Metals* 8(11): p.119–133.
- [15] American Society for Testing and Materials (ASTM). 2003. Standard Test Methods for Flexural Properties of Unreinforced and Reinforced Plastics and Electrical Insulating Materials. *D790-3* 8: p.1–11.